Vision Res. Vol. 24, No. 5, pp. 429–448, 1984
Printed in Great Britain. All rights reserved

0042-6989/84 $3.00 + 0.00
Copyright © 1984 Pergamon Press Ltd

THE VISUAL FIELD REPRESENTATION IN STRIATE CORTEX OF THE MACAQUE MONKEY: ASYMMETRIES, ANISOTROPIES, AND INDIVIDUAL VARIABILITY

DAVID C. VAN ESSEN, WILLIAM T. NEWSOME* and JOHN H. R. MAUNSELL†
Division of Biology 216-76, California Institute of Technology, Pasadena, CA 91125, U.S.A.

(*Received* 6 *June* 1983; *in revised form* 29 *August* 1983)

Abstract—The topographic organization of striate cortex in the macaque was studied using physiological recording techniques. Results were displayed on two-dimensional maps of the cortex, which facilitated the quantitative analysis of various features of the visual representation. The representation was found to be asymmetric, with more cortex devoted to lower than to upper fields. Over much of striate cortex the representation is anisotropic, in that the magnification factor depends upon the direction along which it is measured. There is considerable individual variability in these features as well as in the overall size of striate cortex. Outside the fovea, the cortical representation shows only modest deviations from a logarithmic conformal mapping, in which the magnification factor is proportional to the inverse of eccentricity in the visual field. Comparison of receptive field size with cortical magnification was used to estimate the "point image size" in the cortex (i.e. the extent of cortex concerned with processing inputs from any given point in the visual field). Our evidence supports a previous report that point-image size varies significantly with eccentricity. This is of interest in relation to anatomical evidence that the dimensions of columnar systems in striate cortex are largely independent of eccentricity.

Striate cortex Visual cortex Topography Magnification factor Macaque monkey

INTRODUCTION

It is well established that a topographically organized representation of the visual field is maintained through many stages of processing in the mammalian visual pathway. In general, these topographic representations do not have a uniform emphasis on all parts of the visual field, but instead show a marked overemphasis on the center of gaze. This emphasis on central vision is apparent within the retina itself, where it is manifested most strikingly by large regional differences in the density of retinal ganglion cells. At higher levels, cell density is fairly constant, but there is a large increase in the volume and surface area of tissue devoted to central visual fields (Polyak, 1957).

It is important for several reasons to have accurate descriptions of how the visual field is represented in different cortical areas and subcortical nuclei. Such information allows one to determine what transformations in the sensory representation take place along the visual pathway (e.g. whether there is a progressively greater emphasis on central vision at higher levels). It also allows for interesting comparisons among species, including humans, for which there is physiological or psychophysical evidence concerning the sensory representation at different levels. Lastly, information about visual topography can be combined with data on receptive field size and scatter to yield insights pertaining to the modular organization of cortex (cf. Hubel and Wiesel, 1974).

The present report is a study of the visual field representation in striate cortex of the macaque monkey. There have been several previous studies on this topic, and many of the important features of visual topography in macaque striate cortex are well known (Talbot and Marshall, 1941; Daniel and Whitteridge, 1961; Hubel and Wiesel, 1974; Dow *et al.*, 1981). However, it has proven difficult to map the visual representation accurately and completely in the macaque, in large part because of the convolutions of the cortex. Fully half of striate cortex is buried within the deep, irregular calcarine sulcus.

Many of the difficulties in studying convoluted regions of cortex can be circumvented by the use of two-dimensional representations of the cortical surface. Daniel and Whitteridge (1961) were the first to use such a display to show quantitative aspects of the visual representation over the entire surface of striate cortex. They illustrated a planar projection of a three-dimensional model which was generated on the basis of their measurements of the cortical magnification factor at various eccentricities. This proved to be very helpful in illustrating several important features of visual topography. However, the representation was less than ideal, because it contained substantial distortions of spatial relationships and because it was derived from a limited

*Present address: Laboratory of Sensorimotor Research, Building 10, Room 6C420, NIH, Bethesda, MD 20205, U.S.A.
†Present address: Psychology Department E25-634, MIT, Cambridge, MA 02139, U.S.A.

number of physiological recordings. Recently, a technique was developed for constructing accurate two-dimensional representations of convoluted regions of cerebral cortex using the outlines of histological sections (Van Essen and Maunsell, 1980). With the aid of this technique we have been able to analyze the topographic organization of all but the foveal portion of striate cortex with greater accuracy than heretofore possible. Our results are complementary to the study of Tootell *et al.* (1982), who used the 2-deoxyglucose technique to map the foveal representation with great precision.

In brief, our results confirm and extend previous reports that the emphasis on central vision is considerably greater in striate cortex than in the retinal ganglion cell layer of the macaque. The cortical representation is exceedingly orderly, but it contains unexpectedly large asymmetries and anisotropies. Moreover, there is substantial variability in the size and internal organization of striate cortex in different individuals.

METHODS

Electrophysiology and visual stimulation

Recordings were made from striate cortex in six juvenile macaques (*Macaca fascicularis*) weighing 1.5–3.0 kg. In one experiment (the "main experiment"), recordings were devoted exclusively to the mapping of striate and immediately adjoining extrastriate cortex. In the other experiments the primary objective had been to explore extrastriate cortical regions not related to the present study; the striate recordings were incidental and accordingly were much less extensive. Many of the techniques employed have been described elsewhere (Van Essen *et al.*, 1981; Maunsell and Van Essen, 1983), and only those which are different or which are particularly relevant to the present study are detailed here.

For the recording session each animal was anesthetized with nitrous oxide (70% N_2O, 27.3% O_2, 2.7% CO_2), paralyzed with gallamine triethiodide (7 mg/kg/hr, plus 1 mg/kg/hr D-tubocurarine in the main experiment), and artificially respired through an endotracheal cannula. Recordings were made using lacquer-coated tungsten microelectrodes held in a stepping-motor microdrive. The microdrive was coupled to an $X-Y$ stage mounted on a chamber which in turn was cemented around the margins of an opening in the skull (15 mm dia.). The location of this opening depended on the cortical region to be explored. In the main experiment it was centered on the operculum of striate cortex; electrodes were advanced approximately parallel to the sagittal plane and pointed about 30° downward to provide maximal access to cortex in the calcarine sulcus. In each penetration one or more lesions were made at appropriate depths by passing current through the microelectrode (10 μA × 10 sec). Recordings were made with relatively low-resistance electrodes (0.2–0.8 MΩ at 1 kHz), and most of the receptive field plots were based on multi-unit responses.

The animal's eyes were covered with noncorrective contact lenses and focused with spectacle lenses upon a large screen facing the animal. The optical stimulation system included a projection lamp whose beam passed through a variable-slit diaphragm to provide control of stimulus dimensions and orientation. A pair of galvanometer-controlled mirrors was used to reflect the beam onto any desired location on the screen.

Projection screen and coordinate transformations

Because the representation of the entire visual hemifield was being explored, a simple tangent screen was not satisfactory for these experiments. Instead, we used a composite screen consisting of three vertical faces, each extending from floor to ceiling. Each face was positioned so that it was tangent to an imaginary sphere of radius 113 cm and centered on the midpoint between the animal's eyes. Receptive fields were drawn onto sheets of paper attached to the screen. At the end of the experiment the location of each receptive field center was determined with respect to coordinates on the relevant screen face. In the main experiment this information, along with receptive field dimensions, identifying characteristics of the recording sites, and screen coordinates for the foveal projection of each eye, was entered into a computer (PDP 11/34A). Using a set of transformations appropriate for our particular screen configuration, each receptive field location was then translated into coordinates of eccentricity and polar angle (i.e. in spherical polar coordinates with axis along the direction of gaze for the corresponding eye). For the primate visual pathway, with its strong emphasis on central vision, we find this coordinate system to be much preferable over other systems, such as those involving azimuthal and elevational coordinates (cf. Bishop *et al.*, 1962).

Monitoring of eye position

In general, physiological mapping of visual topography is subject to various sources of error associated with determination of receptive field locations on the projection screen and with determination of retinal axes with respect to screen coordinates. In striate cortex, receptive field boundaries were usually quite sharp, and the uncertainty in the location of receptive field centers on the screen was usually only 0.1°–0.2° near the center of gaze and less than 1° even in the far periphery. The uncertainties in relating screen coordinates to retinal coordinates are generally larger than this, and they deserve explicit consideration. Significant errors can occur at several stages, including the visualization of the center of the fovea, the projection of this point onto the screen, compensation for cyclorotation of the eyes, and the detection of eye movements during the experiment.

The projections of the fovea and the optic disk of each eye were determined using a reversing-beam ophthalmoscope. The foveal region, identifiable by its macular pigmentation and vascular pattern, is about 4° across in the macaque (Polyak, 1957; Rolls and Cowey, 1970); its center could be determined to within about 0.5°. In addition, the mechanical swivel on the ophthalmoscope was only accurate to about 0.5°. When several determinations were averaged, the absolute error in estimating the projection of each fovea onto the screen was somewhat less than 1°. This error was reduced by using the screen coordinates of left eye and right eye receptive fields for binocularly-driven neurons in or near the foveal representation. Since the majority of binocularly driven striate neurons have receptive fields in close correspondence for the two eyes (Poggio and Fischer, 1977), the separation of small monocular fields on the screen is an accurate measure of true binocular misalignment and thus provides a basis of adjusting the ophthalmoscopically determined foveal projections. After this compensation we estimate that the remaining uncertainty in the projection of each fovea was about 0.5°.

Eye movements during the course of physiological recordings were monitored in two ways. The projections of the foveas were checked regularly, usually at the beginning of each microelectrode penetration. In some cases, there was no detectable drift over the duration of the entire experiment, but more commonly there were gradual shifts, not exceeding 1°/hr. As an additional check on the stability of eye position, we occasionally plotted receptive fields twice for the same recording site, once as the microelectrode was being advanced, and a second time when the electrode reached the same depth as it was being retracted 1–2 hr later. Shifts in receptive field location were usually negligible, indicating that eye movements during the course of individual penetrations were not a major problem.

Several approaches were used to assess the degree of ocular cyclorotation at the time of the physiological recordings. The simplest measure involved comparing the projections of the optic disc and the fovea, since the center of the optic disc lies just dorsal to the horizontal meridian on the retina (Malpeli and Baker, 1975). We consistently found the projection of the optic disc to be on or just below a horzontal line running through the projection of the fovea for each eye, which indicates that there was little ocular cyclorotation in the paralyzed state. In the main experiment, two more sensitive measures of cyclorotation indicated that there was actually a slight intortion of the eyes. The first involved measurements of receptive fields for recording sites at the V1/V2 border. For each eye, the orientation of the "zero azimuthal meridian" (the line dividing the ipsilateral and contralateral hemiretinae), can be determined from the absolute alignment of receptive fields recorded at widely separated sites along the V1/V2 border (Cooper and Pettigrew, 1979). In the main experiment, the alignment of receptive fields for the five recording sites at the V1/V2 border indicated an intorsion of 1° for each eye. This was confirmed by measurements of apparent receptive field disparities after correction for translational misalignments. Receptive fields in the inferior quadrant had systematic uncrossed disparities, while those in the superior quadrant mostly had crossed disparities and those near the horizontal meridian showed vertical misalignment. The difference in rotational alignment was estimated to be 2°. In the subsequent analysis all receptive field locations were corrected for this cyclorotation.

Histology

After completion of the recording session, the animal was sacrificed and the brain processed for histology using techniques standard for this laboratory (Van Essen *et al.*, 1981, 1982). Electrode tracks and other histological data were plotted on photographs of sections enlarged to a final magnification of × 8 after correction of 16% shrinkage during histological processing. In order to assess whether there was significant shrinkage of the brain during the initial fixation, we compared the depth of lesions as they appeared on the photographic enlargements with the depth of the microelectrode noted at the time the lesion was made. An additional check was to compare the separation between widely-spaced electrode tracks, as judged from the readings on the $X-Y$ stage for the recording chamber, with their separation in the processed tissue. Both sets of measurements indicated that in the main experiment the fixed, unsectioned brain was slightly smaller than in the living state (about 8% linear shrinkage). We did not introduce any correction factor for this initial shrinkage, however.

Cortical maps

Two-dimensional maps of striate cortex were made using a procedure described in detail elsewhere (Van Essen and Maunsell, 1980). In brief, the outline of layer IVc was traced from photographic enlargements of sections taken at regular intervals through the region of interest. To form the cortical map, the outlines were traced onto a single sheet of paper with an appropariate degree of straightening of each contour as needed to obtain correct alignment. The key to construction of a satisfactory map is to change the shape, but not the length, of each outline in such a way that proper spacing between neighboring contours is always maintained.

The accuracy of the mapping procedure was of critical importance in the present study, because we wanted to minimize errors in the determination of both surface area and linear distances throughout the cortical map. The technique for constructing two-dimensional maps can be used in a routine fashion to represent surface area to within 20–30%, but without

special precautions the distortions in linear relationships are often greater, reaching 50% or more in regions where the cortex has a substantial degree of local intrinsic curvature. In the main experiment a major effort was made to minimize all types of distortion and also to obtain quantitative estimates of the magnitude of the residual distortions, using a procedure described previously (Appendix to Van Essen and Maunsell, 1980). Figure 1(A) shows the map of striate cortex in the main experiment. The map was constructed from the outlines of sections taken at 1 mm intervals. The thin contour lines

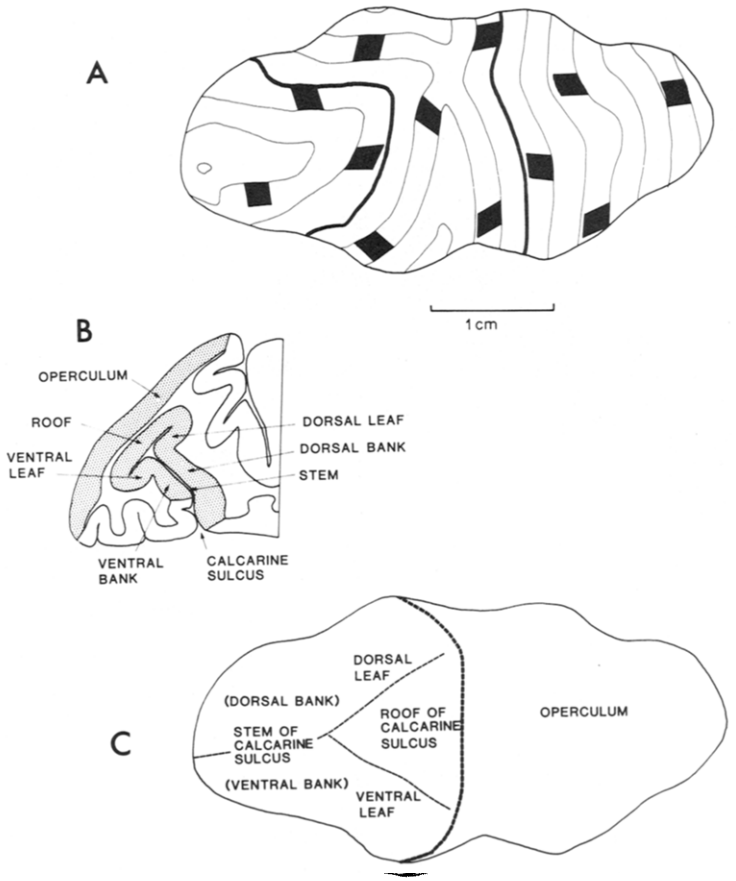

Fig. 1. A two-dimensional map of striate cortex from the main recording experiment. (A) A version of the map containing contour lines from sections spaced at 2 mm intervals. Darkened regions indicate the representation of "test squares" on map. The procedure for their delineation is as follows. Two points separated by exactly 2 mm were marked along the contour of layer IV in one section, thereby designating two corners of the square. Another pair of points was marked in corresponding locations on a section 2 mm away from the first. In cases where the plane of sectioning was normal to this part of the cortical surface, this second pair of points served as the other two corners of the test square, as they were exactly 2 mm away from the first. In other cases, the sectioning plane was oblique to the local orientation of the cortex, and hence the actual distance between corresponding points on the two sections was greater than 2 mm. This distance was calculated by placing the section outlines in precise registration (i.e. as they were in the intact hemisphere), measuring the offset parallel to the sectioning plane of corresponding points on the two sections, and calculating the actual separation between points as the hypotenuse of a right triangle whose sides were now known. Given this value, it was then possible to calculate the fractional separation between corresponding points that equalled 2 mm and to work these fractional distances on the map to denote the remaining two corners of the test squares. Planimetric measurements were then used to determine the actual surface area of each of the test squares. The total surface area of striate cortex determined from this map was 690 mm^2. (B) Outline of a parasagittal section approximately 5 mm from the medial edge of the hemisphere. Stippling indicates the extent of striate cortex on the operculum and in the calcarine sulcus. (C) An outline of the same cortical map as in A, with major geographical features noted. The smooth external operculum is to the right of the heavy dashed line and the calcarine sulcus to the left. Calcarine cortex has the configuration of a mushroom lying on its side, with a "stem" and a "head" each consisting of two sheets of cortex. The stem, to the left of the map, has dorsal and ventral banks joined along the fundus of the calcarine sulcus. The head of the mushroom has a "roof" and two "leaves" joined to the roof along separate branches of the Y-shaped fundus. The original three-dimensional configuration of striate cortex can be reapproximated by tracing the map onto a sheet of paper, cutting it out, making creases along each dashed line, and then folding along the creases, in the manner originally suggested by Daniel and Whitteridge (1961).

represent the outlines of sections at 2 mm intervals, i.e. every other one used in the construction. For purposes of orientation, Fig. 1(B) shows the outline of a representative section, corresponding to the heavy contour in part A. Striate cortex has been stippled, and various geographical regions (the operculum and different parts of the calcarine sulcus) are indicated. Figure 1(C) shows these regions as they appear on the cortical map. Cortex to the left of the heavy dashed line lies within the calcarine sulcus. After unfolding, the fundus of this sulcus has a Y-shaped configuration, as denoted by the fine dashed line. Note that where the smooth cortex of the operculum is represented, the contour lines in Fig. 1(A) are oriented roughly vertically and parallel to one another, as would be expected for parasagittal sections through this region.

In order to illustrate the accuracy of this particular cortical map, 12 different test areas were selected, each of which was determined to be square and 2 mm on a side in the intact hemisphere (see figure legend). If the cortical map were perfect in all respects, the representation of these test squares would be identical to that within the intact hemisphere, namely, squares 2 mm on a side. In the actual map, the distortions are in all instances reasonably small. The estimated areal distortions are nowhere more than 10%, and the linear distortions are 7% on average and nowhere more than 20%. Clearly, there is a noticeable degree of angular distortion in a few places, but in the worst instance there is a deviation of only 30° in the mapping of the corners of the test square. Moreover, spot checks in other parts of the map indicate that the quality of the represention is uniformly high and has not been substantially misrepresented by our particular choice of test squares.

Data analysis

A number of different computer analyses were carried out on the data from the main experiment in order to determine topographic contours, magnification factors, etc. Relevant details of the analysis routines are provided in the text and/or the appropriate figure legends.

RESULTS

A detailed mapping of striate cortex topography

We shall first describe the results for the main experiment, in which extensive recordings were made over a widespread portion of striate cortex. In this experiment 22 microelectrode penetrations were made, all oriented approximately in the parasagittal plane and all but 5 extending from the operculum of striate cortex into the calcarine sulcus. A total of 156 recording sites were assigned to striate cortex on the basis of histological identification of microelectrode tracks and lesions; an additional 45 sites were in extrastriate cortex, mainly in V2.

Many of the basic features of visual topography in striate cortex can be illustrated qualitatively by examining results from a single microelectrode penetration, as shown in Fig. 2. The section containing the electrode track was approximately midway across the hemisphere, as indicated on the dorsal view in Fig. 2(A). The course of the electrode track is indicated in Fig. 2(B), with each recording site denoted by a tic mark. Figure 2(C) shows the same two-dimensional map of striate cortex illustrated in the preceding figure; also indicated on the map are contour lines from the section containing the electrode track (heavy solid lines) and the locations of recording sites from this penetration. Finally, Fig. 2(D) shows the receptive field locations within the contralateral visual hemifield for the various recording sites in this penetration. Altogether, there were 21 recording sites, the first 17 of which were in striate cortex [stippled region in Fig. 2(B)] and the remaining 4 in V2 on the ventral bank of the calcarine sulcus. As expected from previous studies of striate cortex topography, the recording site on the operculum (Site 1, to the right on the cortical map) had a small receptive field within a few degrees of the fovea. As the electrode was advanced through the dorsal bank of the calcarine sulcus (Sites 2–10), the receptive fields encountered were larger and farther from the fovea. Between sites 10 and 11 the electrode crossed to the ventral bank of the sulcus, and the receptive field progression shifted from the inferior quadrant, close to the horizontal meridian, to the superior quadrant, close to the vertical meridian. Surprisingly, field 11 was significantly closer to the fovea than field 10 (18° vs 29° eccentricity) despite the greater distance of site 11 than site 10 from the foveal representation on the section [Fig. 2(B)] and on the cortical map [Fig. 2(C)]. As the electrode progressed towards the V1/V2 border (sites 11–17), receptive fields approached the vertical meridian, but there was no encroachment into the ipsilateral hemifield for sites within striate cortex. Once the electrode passed into V2, the progression of receptive field centers immediately reversed (sites 18–21). With equal abruptness, receptive fields became several times larger. For the sites closest to the V1/V2 border there was a significant, albeit small, extension of receptive field margins into the ipsilateral hemifield. A noteworthy feature of the recording sequence in striate cortex is the relatively small degree of receptive field overlap for adjacent recording sites, which were only 0.5 mm apart. For separations of 1 mm, i.e. every other site, there is no overlap of receptive fields whatsoever. This is a lower value for the cortical distance needed to avoid overlap than has been reported elsewhere, as will be discussed in greater detail below.

In the remainder of this paper we will rely almost exclusively on cortical maps to display information about recording sites and visual topography in striate cortex, thereby avoiding the complexity of showing an inordinately large number of section outlines. The

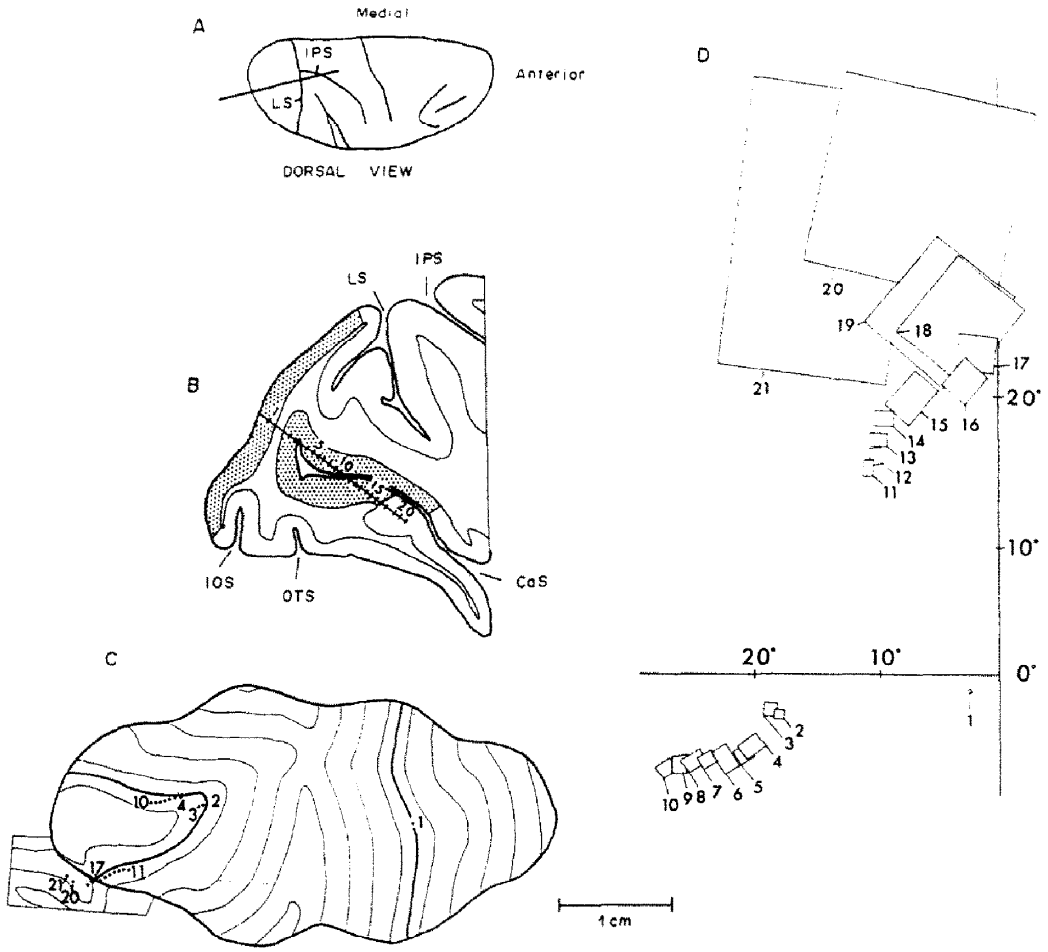

Fig. 2. A representative penetration through striate cortex. The parasagittal section in (B) was taken at the medio-lateral location indicated in the hemisphere drawing in (A) Twenty-one recording sites in a single penetration are indicated on the section outlined in (B) and on the cortical map in (C). Heavy solid lines on the map represent the outline of the section in (B). Note that many of the recording sites on the map fall slightly off the contour for this section. This is partly because the electrode track was not exactly parallel to the sectioning plane, but more importantly because some of the recording sites in superficial layers projected onto layer IV of more distant sections because of the oblique orientation of radial columns in the cortex. (D) Shows the receptive fields for all 21 recording sites in this penetration.

locations of all 156 recording sites within striate cortex are shown in Fig. 3(A). Receptive field centers (or, for binocular responses, the mid-points between left-eye and right-eye field centers) are shown in Fig. 3(B). For ease in interpreting these results, most of the recordings have been connected into sequences, each from a few penetrations, which run along roughly straight courses within the cortical map. Each sequence (A–A′, B–B′, etc.) starts at the margin of striate cortex in the calcarine sulcus, to the left on the map, and terminates a centimeter or more to the right. In the visual field each sequence starts either along the vertical meridian (A, B, E–G) or in the far periphery (C, D) and curves towards the horizontal meridian and fovea.

One important feature of the cortical representation evident in this illustration is that smooth sequences of recording sites within the cortex invariably correspond to smooth progressions of receptive field centers. Thus, at this level of resolution the cortical representation preserves all neighborhood relationships within the visual hemifield and can be regarded as a first-order transformation of the visual field in the sense defined by Allman and Kaas (1971). Moreover, the representation is highly regular, insofar as there is an orderly spacing between receptive field centers for recording sequences in which the sampling was at fairly constant intervals (e.g., C–C′). For such sequences, the deviations from a perfectly smooth progression are no greater than the dimensions of receptive fields (drawn in for a few of the recording sites), and they can be attributed to the scatter in receptive field locations encountered in radial penetrations through the cortex (Hubel and Wiesel, 1974).

The results from this experiment have been summarized in Fig. 4 by plotting lines of constant eccentricity (iso-eccentricity contours) and constant polar angle (iso-polar contours) for all except the foveal representation in striate cortex. The iso-eccentricity

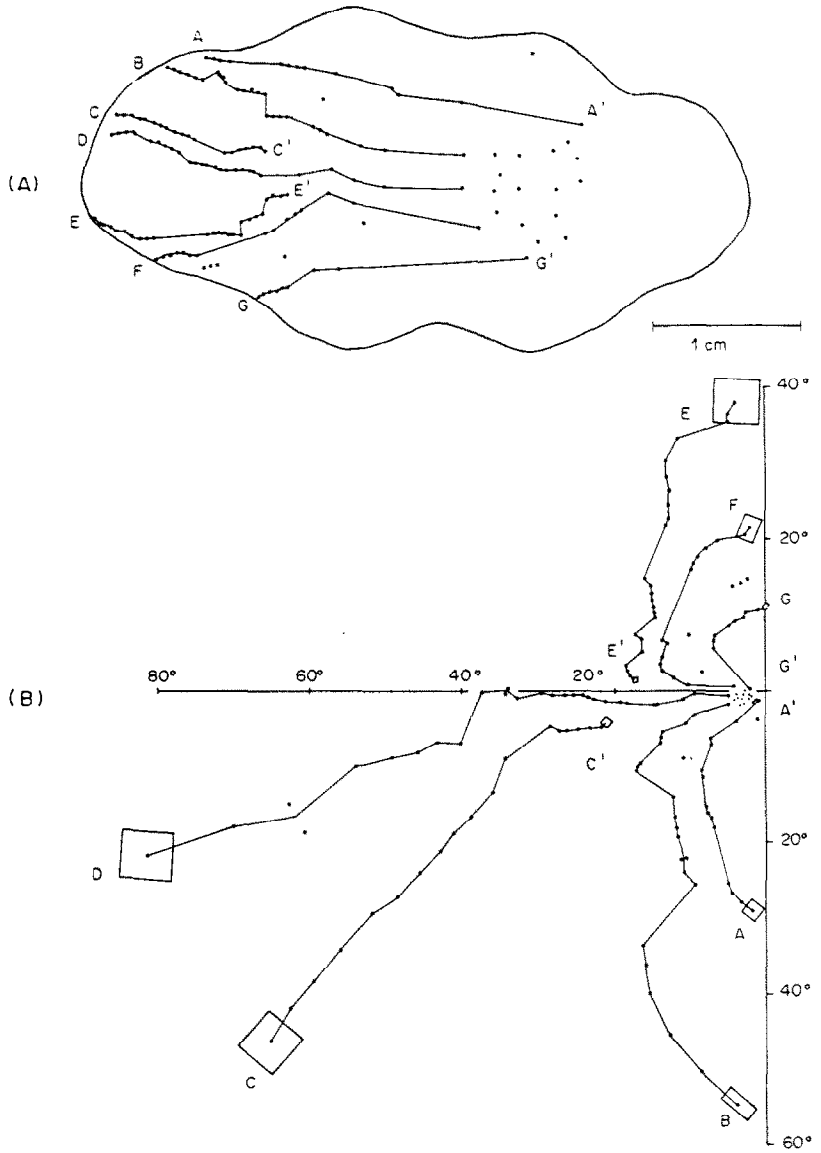

Fig. 3. (A) The location of all 156 recording sites within striate cortex. Lines A–G connect sequences running approximately left-to-right across the map. (B) Receptive field centers for these recording sites, grouped in identical fashion. Receptive field outlines are shown for the first member of each sequence, and also for the last member in two (C′ and E′). Receptive fields at the central ends of the other sequences were too small to be represented accurately in the figure. At a few recording sites, separate receptive fields were plotted for two distinct units or for a single unit and the multi-unit background. In these cases the line for the field progression sequence was drawn midway between the two field centers.

contours chosen for this figure span the range from 2.5° to 80° and are spaced at intervals of a factor of two. For central visual fields, the contours run aproximately vertically from top to bottom on the map, but they become curved and oblique at higher eccentricities. The iso-polar contours are represented at intervals of 45° polar angle between the inferior vertical meridian (0°, top of map) and the superior vertical meridian (180°, bottom of map). They run approximately horizontally on the cortical map and thus intersect the iso-eccentricity contours roughly at right angles.

Several other landmarks of visual topography have been indicated on the cortical map. The foveal representation (central 2°) is indicated by asterisks. The margin of the far periphery, i.e. that portion of the visual perimeter not along the vertical meridian, is denoted by solid triangles. The region in which exclusively monocular responses were obtained is stippled on the cortical map and in the visual field. This region is somewhat larger than the anatomically defined monocular segment (see legend to Fig. 4).

Adjoining the monocular segment is a narrow strip of cortex, the prostriate area, which is thinner and more lightly myelinated than V2 and which lacks callosal inputs along the border with striate cortex

(Van Essen *et al.*, 1982). In the one penetration that passed through the prostriate area (an extension of sequence C in Fig. 3), we elicited weak responses to stimuli in the periphery of the visual field at three successive recording sites. Even though the responses were not crisp enough to plot well-defined receptive fields, these results are significant in suggesting that the prostriate area is a visually responsive subdivision of cortex.

Before discussing the representation in striate cortex in greater detail, it is important to consider the various factors contributing to the uncertainty limits shown for each of the topographic contours in Fig. 4. The first is the intrinsic scatter in receptive field locations at any given recording site. Hubel and Wiesel (1974) showed that receptive field scatter is comparable to receptive field size over much of striate cortex. We generally found less scatter than this for receptive field plots of closely spaced recording sites, presumably because most of our recordings were from multi-unit clusters. Hence, it is likely that receptive field scatter introduced only small errors, 0.25 mm or less, in our assignments of topographic contours. The second factor is the low density of recording sites in some parts of the cortex. The errors associated with sampling density are negligible in regions where there were one or more recording sites per square millimeter of cortical surface, as was the case over much of the calcarine sulcus. In other regions, however, it was necessary to interpolate or extrapolate over substantial distances (6–8 mm; see figure legend) in order to estimate contour locations. This contributes uncertainties of up to 1 mm in places. The third source of error derives from the uncertainty of about 0.5° in our estimate of the projection of each fovea (see Methods). The contribution of this factor is inversely proportional to eccentricity, and hence, the uncertainty limits are largest near the foveal representation (approx. ± 1 mm at 2.5°).

Several important features of striate cortex topography can be discerned from inspection of Fig. 4. The pronounced emphasis on central vision is obvious, as more than half of striate cortex is devoted to eccentricities of less than 10°. Although the iso-eccentricity and iso-polar contours are laid out in a relatively orderly fashion on the map, there are several significant irregularities and asymmetries. The asymmetric arrangement of iso-eccentricity contours, especially in the periphery, has already been mentioned in relation to Fig. 2. It is also apparent that there is a slightly greater representation of inferior fields than of superior fields and a substantially greater representation of fields within 45° of the horizontal meridian (45°–135° polar angle) relative to fields within 45° of the vertical meridian (0°–45° and 135°–180° polar angle).

Cortical magnification factors

In order to provide a quantitiative assessment of

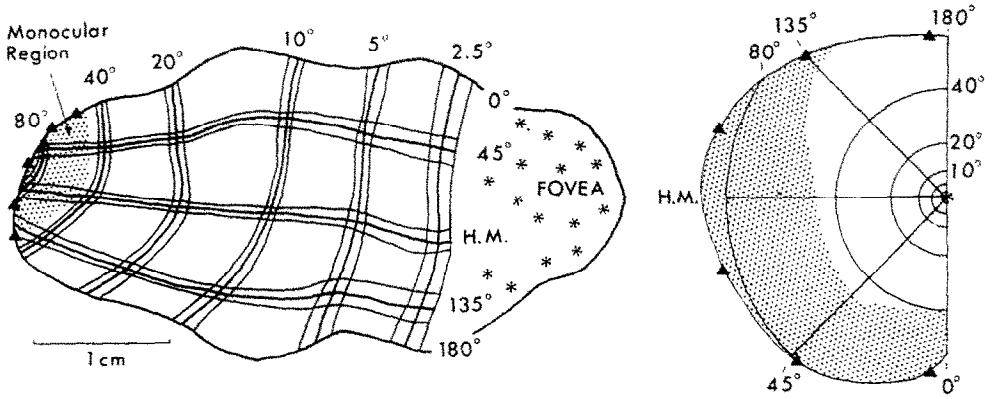

Fig. 4. The location of iso-eccentricity and iso-polar contours in striate cortex of the main experiment. The locations of these contours were determined using a computer program to interpolate or extrapolate over limited distances. The computer first searched for all pairs of recording sites separated by less than 8 mm. To determine the location of any given isoeccentricity contour, it then selected all pairs in which one or both receptive fields were within 30% of the desired eccentricity. By interpolation or extrapolation from each pair over a limited distance, the location of a family of points on this contour could be predicted. In making the interpolation or extrapolation, it was assumed that the X-coordinate on the map was proportional to the logarithm of eccentricity and that the Y-coordinate was independent of eccentricity. For iso-polar contours, a similar procedure was carried out, starting by selecting pairs in which one or both receptive fields were within 20° of the desired polar angle. Interpolation and extrapolation were based on the assumption that the Y-coordinate was linearly proportional to the polar angle and the X-coordinate independent of it. None of these assumptions is perfectly true, but we inferred that they were reasonably accurate, based on the rather limited scatter seen for the points used to predict the various contours. Stippling denotes the region in which exclusively contralateral (left-eye) responses were obtained. This "monocular region" was determined from recordings while the eyes were directed straight ahead, and it in part reflects the obstruction of the field of view by the nose. The true monocular segment completely lacks anatomical inputs from the ipsilateral eye and cannot be driven binocularly even when the eyes are deviated to the ipsilateral side; it is somewhat smaller than the region indicated here.

topographic organization, Daniel and Whitteridge (1961) introduced the notion of the "magnification factor" to describe the visual representation in striate cortex. Their particular expression for magnification was a linear measure (mm of cortex per degree of visual field), i.e. a comparison of distances along two surfaces. Magnification can equally well be expressed as an areal measure, mm^2 of cortex per deg^2 of visual field (Myerson *et al.*, 1977; Tusa *et al.*, 1978). In fact, the two expressions for magnification provide somewhat different types of information about the sensory representation, and it is useful to determine both linear and areal magnification factors for any given visual area. The areal magnification factor reflects the total amount of cortex (as well as the total number of cells, if cortical thickness and average cell density are constant) devoted to a given part of the visual field. The linear magnification factor is a more complex measure, insofar as it is a function not only of location in the cortex, but also of the direction along which it is measured. If the linear magnification factor varies with direction about a given point, the representation at that point is, by definition, anisotropic. Information about linear magnification provides a convenient basis for assessing local distortions in the sensory representation.

Daniel and Whitteridge (1961) made three important observations concerning the magnification factor in striate cortex of the macaque and baboon. They found that to a first approximation the linear magnification factor was: (1) proportional to the inverse of retinal eccentricity; (2) independent of polar angle (i.e. the same wherever measured along any given iso-eccentricity contour); and (3) independent of the direction within the cortex along which it was measured (i.e. isotropic). Interestingly, there is only one type of mathematical transformation which exactly satisfies these three conditions. This is the logarithmic conformal mapping (Fischer, 1973; Schwartz, 1977). In such a representation, distance in the cortex is proportional to the integral of cortical magnification. Along the axis corresponding to constant polar angle, magnification is inversely proportional to eccentricity, and hence distance is proportional to the logarithm of eccentricity ($x \propto \log E$). Along the other axis, corresponding to constant eccentricity, magnification is constant, and hence distance is proportional to polar angle ($y \propto \theta$). It would be impossible for striate cortex to contain a perfect logarithmic conformal mapping of the entire visual hemifield, as the foveal representation would then be infinite in extent. However, it is clearly of interest to know just how closely striate cortex conforms to such a straightforward and convenient description. One way of assessing this is to examine the transformation onto the cortical map of certain appropriately chosen contour patterns in the visual field. Figure 5 shows such a pattern, in which the visual field (right) is divided into a "spiderweb" by a series of iso-eccentricity and iso-polar contours. The contours were chosen in such a way that the compartments in the visual field are all identical in shape and are proportional to the square of eccentricity in size. If striate cortex contained a true logarithmic conformal mapping, these compartments would all map onto squares of equal size in the cortex. On the left is the representation of this pattern on the map of striate cortex from the main experiment. Solid lines denote regions in which the density of nearby recording sites was high enough to permit accurate localization of contours; dashed lines denote regions in which interpolation or extrapolation over greater distances was necessary. There are several major points to be made in relation to the size and shape of these compartments. The areal magnification factor is equal to the ratio of surface areas of corresponding

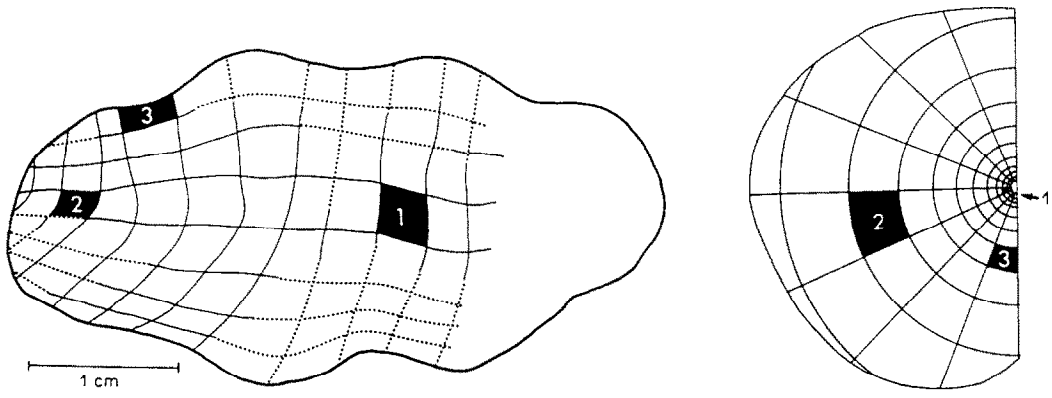

Fig. 5. Transformation of visual field compartments onto the cortical map. Compartments in the visual field, each proportional to the square of eccentricity, map onto cortical compartments that are roughly constant in size and shape over most of striate cortex. Those in the peripheral representation (left) tend to be somewhat smaller than those representing central fields, however, and those close to the representation of the superior vertical meridian (below on the map) are highly elongated. Solid contours represent the most accurate portion of the map; broken contours indicate less accuracy because of lower density of recording sites.

cortical and visual field compartments. Thus in regions where the cortical compartments are fairly constant in size, such as along much of the horizontal meridian, areal magnification must be proportional to the inverse square of eccentricity. At large eccentricities the compartments are significantly smaller, however, so the overall relationship must be somewhat steeper than a simple inverse square. This means that the average linear magnification factor, which is the square root of the areal magnification factor, is not strictly proportional to the inverse of eccentricity, so the first of the three conditions for a logarithmic conformal mapping is not exactly satisfied. Moreover, there are consistent differences in the sizes of the cortical compartments at any given eccentricity range, with the largest ones generally along the horizontal meridian and the smallest along the vertical meridian. Thus, the second condition (independence of polar angle) is not met either.

The question of whether magnification depends on direction within the cortex can be addressed by comparing the shape of the visual field compartments, which are all nearly square, with the corresponding cortical compartments, which are approximately square in some regions but highly elongated in others. Where the cortical compartments are square, it can be inferred that the representation is locally isotropic, or conformal, and the linear magnification factor (distance in cortex divided by distance in the visual field) is independent of local direction. This is true along most of the horizontal meridian representation, for example. However, in other regions, particularly along the superior vertical meridian, the magnification is greater along iso-polar contours than along iso-eccentricity contours, and the representation is locally anisotropic. Hence, the last of the three conditions for a logarithmic conformal mapping is met only for a limited portion of cortex. Interestingly, it is only the magnification along iso-eccentricity contours, M_e, which depends markedly on polar angle; the magnification along iso-polar contours, M_p, is relatively constant for each eccentricity range. The "anisotropy index", M_p/M_e, is near unity along the horizontal meridian, but has values between 1.5 and 3.0 along most of the superior vertical meridian and between 1.0 and 2.0 along the inferior vertical meridian.

In order to specify some of these features of the visual representation more quantitatively, linear and areal magnification factors were calculated for all of extrafoveal striate cortex by comparing the dimensions of cortical compartments with those of the corresponding visual field compartments. Figure 6 shows log–log plots of all three measures of cortical magnification, M_p, M_e, and M_a, as functions of retinal eccentricity. For eccentricities of 2.5° and above, each set of data is reasonably well fit by a linear least-squares regression whose slope denotes the exponent of the best-fitting power function relating magnification to eccentricity. These relationships are

$$M_p = 12.0\ E^{-1.15}\ \text{mm/deg} \quad (1)$$

$$M_e = 9.0\ E^{-1.15}\ \text{mm/deg} \quad (2)$$

$$M_a = 103\ E^{-2.28}\ \text{mm}^2/\text{deg}^2 \quad (3)$$
$$(\text{for } E > 2.5^\circ).$$

The areal magnification, M_a, is approximately equal to the product of M_e and M_p, although this relationship is exact only in regions where the contours interesect precisely at right angles. As expected from the qualitative considerations already mentioned, the magnification factors show a slightly greater dependence on eccentricity than would be expected from a pure logarithmic conformal mapping, for which the exponents would be -1 for linear magnification and -2 for areal magnification. The expressions for M_e and M_p have nearly identical exponents, but they differ significantly in the scaling factor by which the power function is multiplied. Not surprisingly, there is more scatter in the data points for M_e than for M_p, because of the greater dependence of M_e on polar angle.

Analysis of the foveal representation

Although none of our recordings in the main experiment were directly within the foveal representation in striate cortex, it was nonetheless possible to estimate foveal magnification factors by using information on the size and shape of the cortical map in this region. Planimetric measurements on the map of Fig. 4 indicate that 184 mm² of cortex are devoted to the central 2.5°. This corresponds to an average of 19 mm²/deg² for the central 2.5°, a value which reflects a decreased dependence of magnification on eccentricity in the foveal region. If an assumption is made about the general form of this relationship, then a specific value for the peak foveal magnification can be calculated. For example, a mathematically straightforward way suggested by Schwartz (1980) for dealing with the decreased rate of change of magnification in the foveal region is to introduce an additive constant within the previously derived power function [equation (3)] relating magnification to eccentricity:

$$M_a = a(b + E)^{-x} = 103(0.82 + E)^{-2.28}\ \text{mm}^2/\text{deg}^2. \quad (4)$$

The particular value of $b = 0.82°$ is that which was determined to give the appropriate surface area for the representation of the central 2.5° [see legend to Fig. 6(C)]. The shape of this modified power function [equation (4)] is indicated by the dashed line in Fig. 6(C). Although this curve deviates significantly from the straight power function for eccentricities less than 5°, it nonetheless provides an acceptable fit of the data points, as well as meeting the boundary condition relating to total surface area. The peak areal magnification determined from this expression is 160 mm²/deg² at zero eccentricity, declining to 26 mm²/deg² at 1°. Assuming that the foveal representation is isotropic (Guld and Bertulis, 1976), the

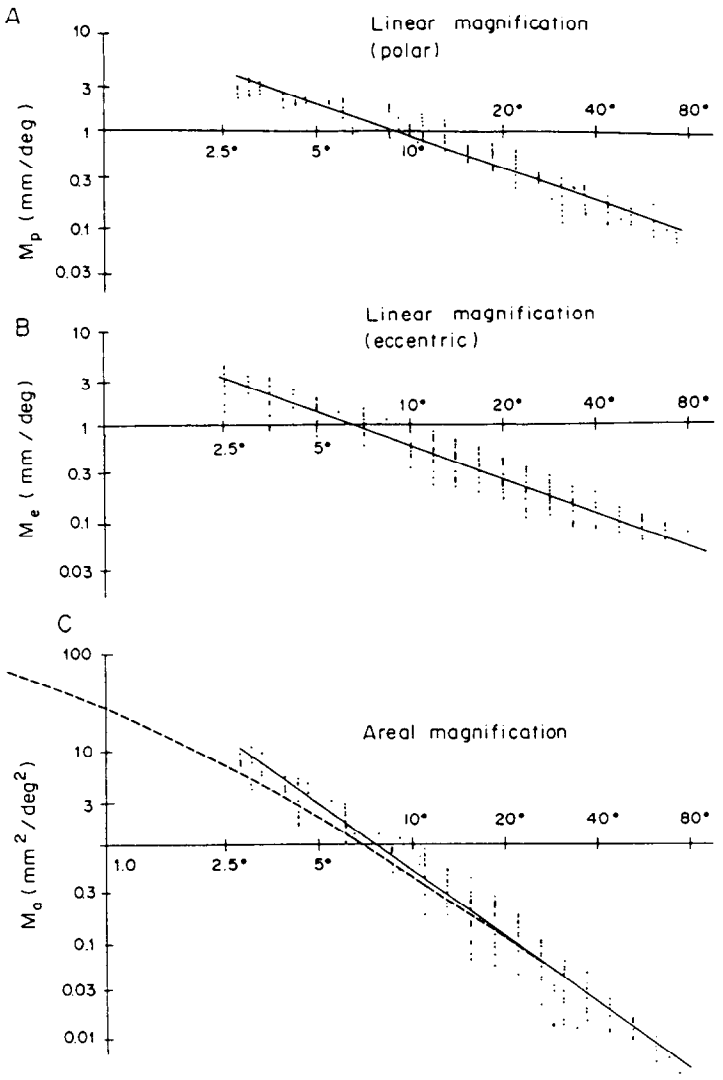

Fig. 6. Cortical magnification as a function of eccentricity. Linear magnification (mm/deg) along iso-polar contours is shown in (A) and along iso-eccentricity contours in (B). Areal magnification is shown in (C). Calculation of magnification factors was based on the topographic contours illustrated in Fig. 5. The map coordinates of the intersections of iso-eccentricity and iso-polar contours were entered into the computer via a graphics tablet. In regions where there was sufficiently detailed information about visual topogrpahy, the spacing of contours was twice as close as that shown in the preceding figure. Regression lines were calculated according to the least-squares method. For each compartment the length of each side was divided by the length of the corresponding visual field compartment to obtain the linear magnification factors (M_e and M_p), and the area of the cortical compartment was divided by the area of the visual field compartment to obtain the areal magnification factor.

calculated linear magnification factors are 13 mm/deg and 5 mm/deg at 0° and 1°, respectively. Obviously, though, the same boundary conditions could be met by expressions of a different general form associated, say, with a flatter curve within the fovea and a sharper change in slope just outside.

Receptive field area vs eccentricity

Hubel and Wiesel (1974) reported that over the eccentricity range of 1–20°, the size of receptive fields in striate cortex (calculated as the square root of receptive field area) was inversely proportional to the linear magnification. Thus, the product of magnification and receptive field size was found to be approximately constant, with a value of about 1 mm. More recently, Dow *et al.* (1981) reported that receptive fields in the foveal representation are consistently larger than predicted from this relationship, with the product of magnification and field size reaching 2–3 mm at eccentricities of 0.1–0.5°.

Our own results on receptive field area as a function of eccentricity from the main experiment are displayed on a log–log plot in Fig. 7(A). Even though nearly all receptive fields were plots of multi-unit responses, there is considerable variability, generally 10-fold or more, in receptive field area at all eccen-

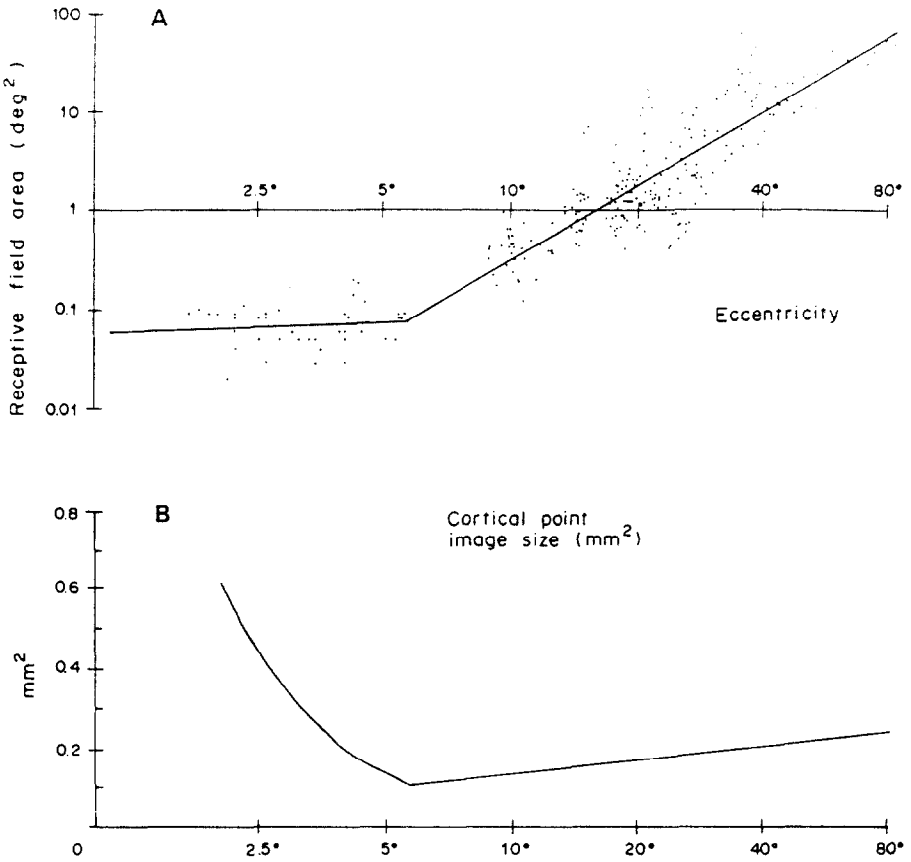

Fig. 7. (A) Receptive field area vs magnification. For binocularly driven responses, separate values are plotted for the left and right eyes. Separate regression lines were calculated for the data above and below 5.5° eccentricity. (B) Cortical point image size (mm^2/deg^2) as a function of eccentricity. The plotted curve equals the product of areal magnification [equation (4)] and multi-unit receptive field area [equation (5)].

tricity ranges, as was found by Dow *et al.* (1981) for the foveal representation as well. Overall, the average field sizes in our data are slightly smaller than those described by Hubel and Wiesel (1974), even though our fields, being from multi-unit responses, should reflect field scatter as well as individual field sizes. At eccentricities greater than 5.5°, the data points are fit by a power function of slope 2.48, similar to but slightly greater than the slope for areal magnification [−2.28, equation (3)]. Below 5.5°, receptive field area shows a markedly reduced dependence on eccentricity, with the best-fitting power function having a slope of only 0.15.

$$\text{R. F. Area} = \begin{cases} 0.057\ E^{0.15} & (E < 5.5^\circ) \\ 0.001^\circ\ E^{2.48} & (E > 5.5^\circ) \end{cases} \quad (5)$$

The decreased dependence on eccentricity near the foveal region might in principle be due to overestimation of the size of the smallest receptive fields, as could occur if the retinal image were blurred by improper focusing or cloudy optics. This is unlikely, however, because we did encounter a few very tiny receptive fields (0.01–0.02 deg^2) with sharp borders, suggesting that image degradation was not a limiting factor in plotting receptive fields. Moreover, our results for low eccentricities are very similar to those obtained by Dow *et al.* (1981) in recordings from alert animals, where focusing was presumably not a problem.

By combining information about receptive field size and cortical magnification, it is possible to estimate the extent of cortex activated by a point of light on the retina—the cortical "point image". The point image is a useful concept for dealing with issues such as the amount of cortex (or the number of cells) involved in processing information from any given point in the visual field. Dow *et al.* (1981) calculated point image size by taking the product of magnification and aggregate field size, where aggregate field size is an expression that reflects the scatter as well as the average size of individual receptive fields. In our situation, the receptive field plots were mostly for multi-unit recordings and were therefore used as a reasonable measure of aggregate field size. Figure 7(B) shows the cortical point image size expressed in terms of cortical surface area (mm^2). Our results indicate that the point image is at a minimum at around 5°, increasing sharply at lower eccentricities and less steeply at higher eccentricities. The shape of this curve is roughly consistent with the

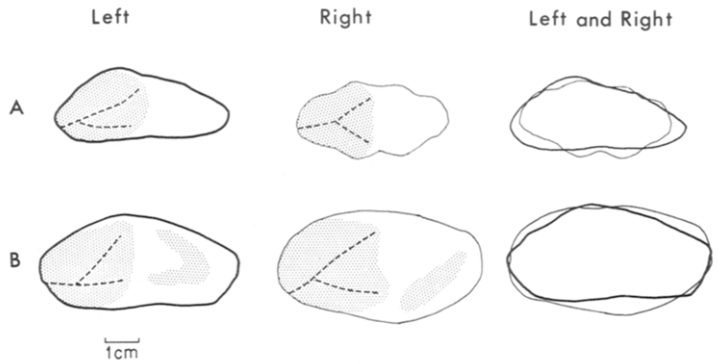

Fig. 8. Individual variability in size and shape of striate cortex. (A) Left and right sides for an animal with an unusually small striate cortex. The right striate cortex was that from the main physiology experiment, already displayed in previous figures. (B) Left and right sides for an animal with a particularly large striate cortex on the right side and a greater-than-average size on the left. Stippling represents cortex buried in the calcarine sulcus (internal or external). Note that an external calcarine sulcus is present in both hemispheres of animal (B) and in neither from animal (A).

results of Hubel and Wiesel (1974), which suggest that point image size is relatively constant outside the foveal representation, and with the results of Dow *et al.* (1981), which suggest that the point image size is considerably larger in the foveal representation than extrafoveally. However, the absolute magnitude of our estimate (0.11–0.6 mm^2) is considerably lower than that obtained in these other reports (1–9 mm^2 over the same eccentricity range). Part of this discrepancy might be related to systematic differences in the criteria used to determine receptive field boundaries, but it seems likely that individual variability in several features of striate cortex organization is also an important factor (see below).

Individual variability

It is obviously of interest to know the degree to which the results from the one hemisphere we mapped in detail are representative of the pattern occurring in other individuals. In the course of various experiments, we have constructed two-dimensional maps of striate cortex in 31 hemispheres from 24 animals, thus providing a substantial basis for assessing individual variability in size and shape. Our results show that the unfolded striate cortex is relatively constant in shape, but quite variable in size, except when the comparison is made between the two hemispheres of the same individual. Figure 8 shows maps of striate cortex near the two extremes of the size spectrum in our sample. The maps in Fig. 8(A) are from an animal with a very small striate cortex on both left and right sides (800 and 690 mm^2, respectively); those in Fig. 8(B) are from an animal in which striate cortex was much larger on both sides (1510 and 1250 mm^2, respectively). In all four cases, as well as in all other hemispheres examined, the unfolded map is approximately elliptical in shape and 1.5 to 2.0 times as long as it is wide. The mean surface area is 1195 mm^2 ($+/-194$ SD, $n = 31$; range 690–1560 mm^2). This is very close to the mean value previously reported for a smaller sample (Van Essen *et al.*, 1981), but the range is larger. The size of striate cortex showed no obvious correlation with body weight over the range in our sample (1.6–3.5 kg). In all seven cases for which we had maps of both right and left striate cortex, the two sides were similar in size, with the smaller side at least 83% and on average 90% of the larger. There was no systematic difference between right and left sides, as the ratio of right/left surface area was 0.98. In most hemispheres with a large striate cortex there was a prominent external calcarine sulcus occupying part of the operculum [cf. Fig. 8(B)].

The large variations in surface area imply that there is individual variability in quantitative aspects of the visual field representation in striate cortex. In principle, the differences could simply be ones of absolute scale. The results from five hemispheres in which limited physiological recordings from striate cortex had been obtained suggest instead that there is significant variability in the relative emphasis on different parts of the visual field. Figure 9 shows maps of striate cortex from four of these hemispheres, plus the one from the main experiment. All maps have been scaled to occupy the same area in the figure; absolute scales representing 1 cm are shown alongside each map. Iso-eccentricity and iso-polar lines are denoted by solid lines for regions where they could be accurately determined. In order to facilitate comparison between hemispheres, each map also shows the location (dotted lines) of contours that would be predicted on the basis of the results from the main experiment. The separation between predicted and actual contours thus provide a measure of the individual differences in topographic organization after compensation for absolute size differences. For some contours the differences are negligible, but for the majority the actual position differs from the predicted by anywhere from a few millimeters to nearly a centimeter. This corresponds to a substantial fraction

of the overall dimensions of striate cortex. Differences greater than 2–3 mm are more than can be accounted for by inaccuracies in the mappings, as was already discussed in relation to Fig. 4. Most of the iso-eccentricity contours are to the right of their predicted location, indicating a decreased emphasis on central relative to peripheral fields, but there are also clear examples of the reverse (e.g. the 2° contour in D). A similar pattern of variability is evident in the location of iso-polar contours. For example, the horizontal meridian is below its predicted location in (C), but above it in (E). This suggests that the slight overemphasis on inferior fields found in the main experiment may be even larger in some hemispheres but nonexistent in others. Overall, some of the individual variability can be ascribed to systematic differences in central vs peripheral or superior vs inferior emphasis. However, it is also necessary to invoke local, nonsystematic differences between individuals.

Despite the fragmentary nature of the recording data, the results from Fig. 9 can even be used to infer that the local anisotropies previously documented for the main experiment also show individual variability. For example, in Fig. 9(C) the separation between 35° and 50° isoeccentricity contours is much greater than in the main experiment, while the separation between the horizontal meridian and the superior vertical meridian is much less. Hence, the average anisotropy in this region must be considerably greater than in the main experiment. A similar analysis applied in Fig. 9(E) to the 30–35° isoeccentricity contours and the

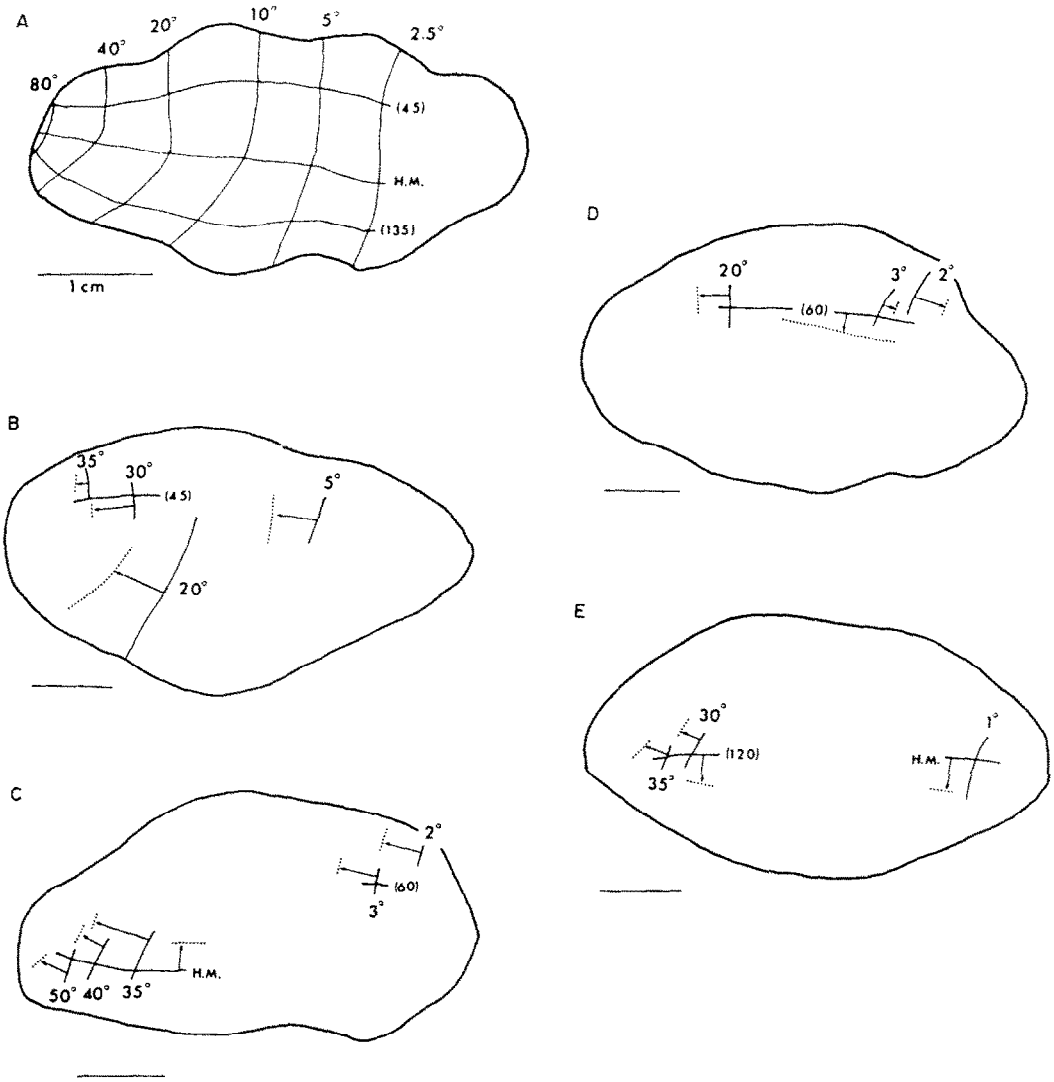

Fig. 9. Individual variability in topographic organization of striate cortex. (A) Topographic contours in striate cortex from the main experiment (cf. Fig. 4). (B)–(E) Striate cortex from four different animals in which partial physiological mapping had been done in experiments designed mainly for exploring other cortical areas. All drawings have been scaled to the same final size. Arrows denote differences between the actual location of a given contour (solid line) and its location predicted from the superposition of the map in (A) (dotted line).

120–180° isopolar contours indicates the opposite result, namely, than in the main experiment the average anisotropy is less than in the main experiment.

In order to summarize these observations on individual variability, we constructed a "standard" map of striate cortex whose surface area equalled that of the mean value of our sample, 1195 mm², and whose shape represents a composite outline of striate cortex, based on the six hemispheres in which physiological mapping data had been obtained. This standard map is used in Fig. 10 to show the approximate range over which various iso-eccentricity contours [Fig. 10(A)] and iso-polar contours [Fig. 10(B)] can be expected to occur. The resultant contour zones are about 5–10 mm wide. In order to derive expressions for magnification vs eccentricity on the standard map, solid lines were drawn through the middle of each contour zone, and a higher resolution version was then constructed by interpolating between these contours. The intersections of iso-eccentricity and iso-polar contours were then processed in the same way as was done for the main experiment (cf. Figs 4–6). The resultant expressions for magnification are

$$M_p = 11.7\ E^{-1.01}\ \text{mm/deg} \quad (6)$$

$$M_e = 13.0\ E^{-1.22}\ \text{mm/deg} \quad (7)$$

$$M_a = 140(0.78 + E)^{-2.20}\ \text{mm}^2/\text{deg}^2. \quad (8)$$

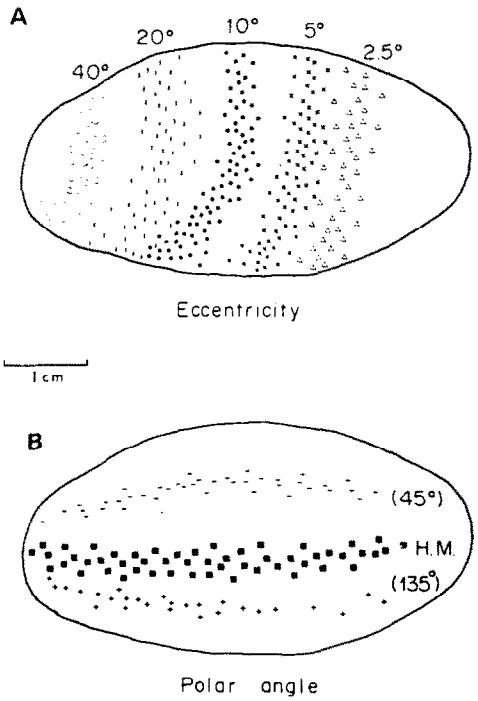

Fig. 10. Visual topography of a "standard" striate cortex. Its outline represents the average shape determined for six hemispheres, five of which are illustrated in the preceding figure. The contour zones represented by the assorted symbols reflect the most likely range for isoeccentricity contours (A) and iso-polar contours (B), based on recording data from the same seven hemispheres.

The expression for areal magnification includes the additive constant needed to provide the correct surface area for the foveal representation [cf. equation (4)]. Overall, the expressions are similar to those obtained for the main experiment. The specific differences are related mainly to the greater size and the slightly lower emphasis on central vision for the standard map relative to that from the main experiment. The magnitude of these differences can be illustrated by noting that the areal magnification at 1° eccentricity is 50% greater for the standard map than for the main experiment (39 mm²/deg² vs 26 mm²/deg²), while at 40° eccentricity it is almost twice as great (0.040 mm²/deg² vs 0.022 mm²/deg²).

Another useful format for representing this information is to translate the data from the standard map of striate cortex onto the outlines of sections cut in different planes, as is shown in Fig 11. Each part of the figure shows a set of three sections through striate cortex, cut in the parasagittal, horizontal, or frontal plane, along with a two-dimensional map of the corresponding striate cortex and a view of the hemisphere showing the levels at which the sections were taken. Indicated on the section outlines are the contour zones for the horizontal meridian and for 2°, 5°, 10°, 20°, and 40° eccentricities. With the aid of this figure, it is possible to take arbitrary sections cut in any of the standard planes and estimate the location of different parts of the visual representation. Of course, such estimates would necessarily be rather approximate, but in view of the marked individual variability of striate cortex, this is inevitable unless recording data are available for the hemisphere in question.

DISCUSSION

In this study we have applied the technique of making two-dimensional cortical maps to the analysis of visual topography in striate cortex, thereby allowing a more detailed characterization of the complete visual representation than heretofore possible. Many of the conclusions of earlier studies have been confirmed, and in addition, new information has been obtained relating to several quantitative and qualitative aspects of topographic organization. It is of particular interest to compare our results with those of other studies with regard to (a) peak magnification factor in the foveal representation; (b) the slope of the power function relating magnification and eccentricity; (c) asymmetries and anisotropies in the representation; and (d) the relation between receptive field area and magnification. Before discussing these topics, though, it is useful to consider the more general issue of individual variability in size and internal organization of striate cortex. Our measurements indicate that there is a more than two-fold range in the surface area of striate cortex (690–1560 mm²). This variability is too large to be accounted for by the inaccuracies of 10–30% in our

mapping technique as it is currently applied (see Fig. 1). A similar range can be inferred from the various individual measurements on macaque striate cortex that have been reported in the literature (Clark, 1941; Chow *et al.*, 1950; Daniel and Whitteridge, 1961). Likewise, a twofold range in surface area has been

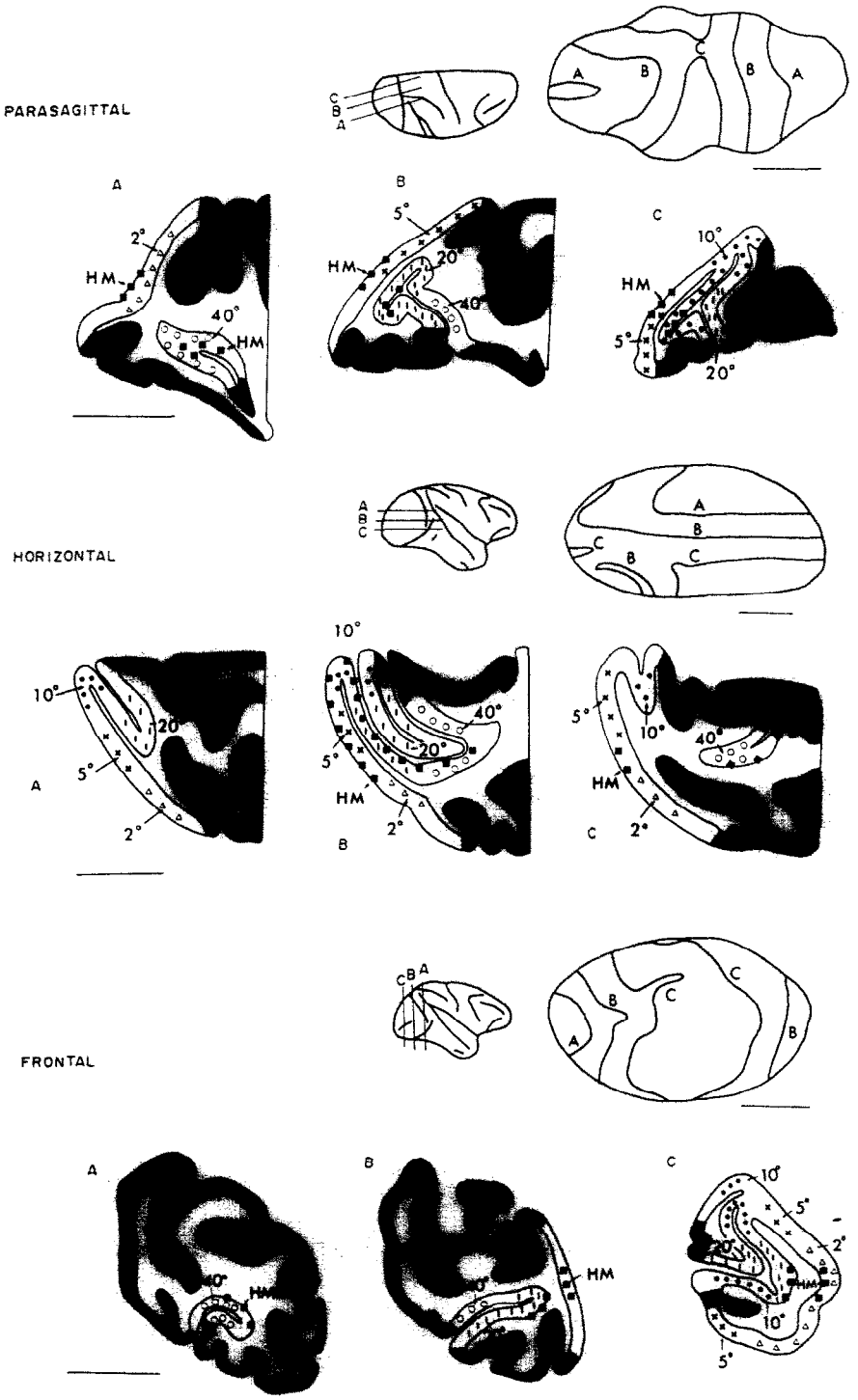

Fig. 11. Visual topography in sections of striate cortex cut in standard sectioning planes. Results are based on the contour zones shown in the standard cortical map of Fig. 10. For each of the three sectioning planes, a map of striate cortex was prepared to the same scale as the standard map. Topographic contour zones for the horizontal meridian and five eccentricities (2°, 5°, 10°, 20°, and 40°) were transferred onto the contours of three representative sections (A, B, and C) on each of the maps. These contour zones were then translated back to the section outlines used in making each map and are indicated by the same symbols as in the preceding figure. Scale bars all 1 cm.

reported for the middle temporal area (MT) in the macaque (Van Essen *et al.*, 1981). In humans, striate cortex is approximately twice as large as in the macque, but the variability is about the same: 1500–3700 mm^2 for the 52 cases reported by Stensaas *et al.* (1974) *and* 2200–2900 mm^2 for the 13 cases reported by Filimonoff (1932).

We also found that the topographic organization of striate cortex shows considerable variability, even after scaling for differences in absolute size. The variability is on the order of 10–15% of the overall extent of striate cortex. Similar observations have been made for other visual areas in the macaque (Van Essen *et al.*, 1981, 1982), for several visual areas in the cat (Tusa *et al.*, 1978, 1979; Donaldson and Whitteridge, 1977), and for somatosensory cortex in several species (Merzenich *et al.*, 1978; Sur *et al.*, 1980, 1981). It is an interesting question whether the variability in size and organization of different sensory areas is correlated with individual differences in various perceptual capabilities.

The foveal magnification factor

Previous estimates of the linear magnification factor for the foveal representation in macaque striate cortex have varied over a seven-fold range, from 4.5 mm/deg (Hubel and Wiesel, 1974) to 30 mm/deg (Talbot and Marshall, 1941; Dow *et al.*, 1981), with intermediate values of 6–13 mm/deg reported in other studies (Daniel and Whitteridge, 1961; Guld and Bertulis, 1976; Hubel and Freeman, 1977; Tootell *et al.*, 1982). This corresponds to nearly a 50-fold variability in areal magnification, which is enormous in comparison to the variability in total surface area of striate cortex. However, it is likely that the actual range of peak foveal magnifications is substantially smaller. The lowest foveal values reported (Hubel and Wiesel, 1974; Daniel and Whitteridge, 1961) are for magnification at around 1° eccentricity, which is sure to be an underestimate of the value at 0°. At the other end of the spectrum, there are several grounds for suspecting that the value of 30 mm/deg may be a significant overestimate. Talbot and Marshall's (1941) figure was based on limited recording data, and insufficient technical detail was presented to ascertain just how accurate the measurements were. Dow *et al.* (1981) based their estimate on extensive recordings from two individuals whose foveal magnification factors evidently differed from one another by about a factor of two. Their estimate of peak foveal magnification involved extrapolation along a line made artifactually steep by these individual differences (see their Fig. 5). Re-evaluation of their data suggests that a peak value of 15–20 mm/deg would be a better estimate. This is in good agreement with the value estimated in the present study, as well as with that obtained by Tootell *et al.* (1982) using deoxyglucose labeling, which is inherently more precise than physiological methods for mapping the foveal representation.

Magnification vs eccentricity

There have been only a few studies in which cortical magnification has been measured over a broad enough range to permit reasonable estimates of the relationship between magnification and eccentricity. Daniel and Whitteridge (1961) showed graphically that there was an approximately inverse relation between linear magnification and eccentricity, but they did not derive an explicit mathematical expression for their data. Schwartz (1977) calculated that the Daniel and Whitteridge data could be fit by a power function whose exponent was −0.9. We have re-examined the same data and found that the exponent is −1.0 if the foveal representation is excluded (because of the known leveling off of magnification at low eccentricities). This value is only slightly different from that obtained in the present study. Hubel and Wiesel found that their data on cortical magnification could be satisfactorily fit using an exponent of −1.0; Gattass *et al.* (1981) calculated an exponent of −1.2. A difference of 0.2 in the exponent is equivalent to a two-fold difference in the relative linear magnification at 2° vs 60° eccentricity, or a four-fold difference in areal magnification. Thus, comparisons among these various studies affirms the conclusion drawn from our own recordings that there are modest individual differences in the relative emphasis on central vs peripheral vision in striate cortex.

The steep dependence of cortical magnification on eccentricity can be dramatically illustrated by comparing the amount of cortex devoted to one square degree of the visual field at extremes of the eccentricity range. For example, the expression for a standard striate cortex [equation (8)] predicts a ratio of 4400 in areal magnification at 1° vs 80° eccentricity (39 mm^2/deg^2 vs 0.0089 mm^2/deg^2). It is instructive to compare this to the ratio of retinal ganglion cell densities at these eccentricities. Because of the lateral displacement of retinal ganglion cells at the fovea it is difficult to determine the precise retinal ganglion cell density at 1°, but the data of Rolls and Cowey (1970) suggest that this value is about 50 times the retinal ganglion cell density at 80°. Thus, the emphasis on central vision is far greater in the cortex than in the retina, as has previously been pointed out by Malpeli and Baker (1975) for the macaque and by Myerson *et al.* (1977) for the owl monkey.

Anisotropies and asymmetries

Our results from the one detailed mapping showed a representation that was remarkably close to isotropic along most of the horizontal meridian. Along the vertical meridian the anisotropies were substantial, but the ratio of maximal to minimal magnification was generally less than a factor of two except for a limited region in the superior periphery. The limited data on other hemispheres suggests that the anisotropies in any given region can be larger in some individuals and smaller in others. Recently,

Sakitt (1982) argued that an approximately two-fold anisotropy must be present throughout the central representation in striate cortex. Her argument was based on the following logic. (1) The expected size and shape of the operculum of striate cortex can be calculated using the expression for magnification as a function of eccentricity derived by Hubel and Freeman (1977). (2) This calculated shape differs markedly from the actual shape of the operculum reported by LeVay *et al.* (1975). (3) Therefore, the assumption of local isotropy used in calculating the theoretical shape must have been wrong (by approximately a factor of two). There are several flaws in this argument, however. The discrepancy between the actual operculum and its calculated version is mainly in absolute size, and not in intrisic shape. Part of this could be attributable to individual differences in the size of striate cortex, as demonstrated in the present study, since the comparison cited by Sakitt (1982) involved data from different animals. Moreover, the size and shape of the calculated version of the operculum is critically dependent on the exact values of magnification in the foveal region, yet this is where the expression used by Hubel and Freeman (1977) is least accurate, as it relies on extrapolation from a limited number of data points. Thus, the discrepancy cited by Sakitt can as readily be attributed to inaccuracies in the estimates of cortical magnification as to the presence of anisotropies in this part of the representation. In any event, neither our results nor those of Tootell *et al.* (1982) support her conclusion, except in the general sense of showing that there are indeed some anisotropies in parts of the visual representation.

Our results indicate that the representation in striate cortex lacks radial symmetry in two important respects: there is a greater emphasis on the horizontal meridian than on the vertical meridian and a slight overemphasis on inferior relative to superior parts of the visual field. Because both biases are small and variable among different individuals, it is not surprising that they have not previously been reported. Whether they are of any functional significance remains to be seen, but similar biases are present at lower levels, including the retina and lateral geniculate nucleus (see Connolly and Van Essen, 1984), and at higher levels, including the middle temporal area (Van Essen *et al.*, 1981; Maunsell and Van Essen, 1983).

Although we have pointed out several ways in which the striate cortex representation deviates from a perfect logarithmic conformal mapping, it is perhaps just as important to bear in mind how modest these deviations actually are. At the very least it is a matter of convenience that the representation can to a first approximation be described by one rather simple equation. Of greater importance is the question of whether there is any functional significance to the logarithmic conformal mapping. Schwartz (1980) has provided several interesting suggestions of how this particular mapping is well suited for the analysis of visual inputs in a highly stereotyped fashion which is largely independent of translational and rotational operations (but see Cavanagh, 1982). It is difficult to envision ways to test this hypothesis in any direct fashion, but hints as to its relevance may come from information on how consistently a logarithmic conformal mapping is found in different areas and in different species.

Receptive field area, magnification, and cortical modules

Hubel and Wiesel (1974) were the first to point out that the close relationship between receptive field size, scatter, and inverse magnification over most of striate cortex may not be entirely fortuitous. Their observations indicated that the cortical point image—the product of cortical magnification and aggregate field size (receptive field size plus scatter)—was roughly 2–3 mm in linear extent. They also noted that this distance is comparable to the dimensions of cortical "hypercolumns"—a pair of ocular dominance columns *or* a complete set of orientation columns. Accordingly, they suggested that striate cortex consists of a large number (*ca* 10^3) of repeating units, or modules, each of which carries out a highly stereotyped analysis of the inputs from a small region of the visual field. The general notion of modular organization has received dramatic support from the discovery of an array of regularly spaced cytochrome oxidase-rich "blobs" in superficial and deep layers of primate striate cortex (Humphrey and Hendrickson, 1980; Horton and Hubel, 1980). These blobs are aligned along the ocular dominance stripes present in layer IV and are spaced at intervals of approximately 0.5 mm.

In the present study we have confirmed and extended the suggestion of Dow *et al.* (1981) that the cortical point image is considerably more variable in extent than Hubel and Wiesel (1974) originally thought on the basis of the data they had available. Expressed in terms of surface area, estimates of cortical point image size range from a minimum of about 0.1 mm^2 (present study) to a maximum of about 70 mm^2 (Dow *et al.*, 1981). Although there are several sources of error associated with these estimates, it is unlikely that these differences of nearly three orders of magnitude are entirely artifactual. Our results clearly indicate a several-fold range of point image size in a single animal, depending on eccentricity in the visual field. That there is individual variability in point image size for any given eccentricity range can be seen by noting the differing extent of receptive field overlap for comparable recording site separations illustrated in various studies (Fig. 2, present study; Figs 2 and 4, Hubel and Wiesel, 1974; Fig. 4, Dow *et al.* (1981). In contrast, there appears to be less variability in the dimensions of hypercolumns and cytochrome oxidase blobs. Ocular dominance stripes vary in width by about a factor of four

over all of striate cortex, but there is no significant difference in the mean spacing for foveal vs extrafoveal cortex, except for a decreased spacing in the far periphery (Connolly *et al.*, 1982; LeVay *et al.*, 1984). The available evidence indicates that comparable variability exists for the spacing of blobs (Horton and Hubel, 1981; Hendrickson *et al.*, 1981).

These considerations by no means invalidate the notion of modular organization in striate cortex. However, they do affirm the importance of ascertaining just what constitutes the fundamental repeating unit within the cortex. Hypercolumns, cytochrome oxidase blobs, and point images offer three conceptually distinct bases for defining modules. We suggest that the point image is the least appropriate of the three. One drawback is that the point image has a complicated shape when examined layer by layer. It is roughly hourglass-shaped, because receptive field size and scatter is lower in layer IVc than in superficial and deep layers. Another drawback is the aforementioned regional and individual variability of point image size.

There are several ways in which hypercolumns and/or cytochrome oxidase blobs could be used to define modules. Whatever the exact configuration of a module, though, its average dimensions are presumably on the order of 0.5 mm on a side. This raises the possibility that there are systematic differences in the number of modules associated with cortical point images in different individuals and in different parts of the visual field. If there indeed are regions where more than one module contributes to the point image, it would be of interest to know whether this multiplicity is a reflection of redundancy or of functional diversity in the underlying cortical circuitry.

Acknowledgements—This work was supported by NIH Grant R01 EY02091, NIH pre-doctoral traineeship NIGMS T32 GM07737 to J.H.R.M., and by the Sloan Foundation. It is a pleasure to thank C. Shotwell for histological work and preparation of figures and C. Hochenedel and C. Oto for typing the manuscript.

REFERENCES

Allman J. M. and Kaas J. H. (1971) Representation of the visual field in striate and adjoining cortex of the owl monkey (*Aotus trivirgatus*). *Brain Res.* **35**, 89–106.

Bishop P. O., Kozak W. and Vakkur G. J. (1962) Some quantitative aspects of the cat's eye: axis and plane of reference, visual field co-ordinates and optics. *J. Physiol.* **163**, 466–502.

Cavanagh P. (1982) Functional size invariance is not provided by the cortical magnification factor. *Vision Res.* **22**, 1409–1412.

Chow K. L., Blum J. S. and Blum R. A. (1950) Cell ratios in the thalamo-cortical visual system of *Macaca mulatta*. *J. comp. Neurol.* **92**, 227–239.

Clark W. E. L. (1941) The laminar organization and cell content of the lateral geniculate body in the monkey. *J. Anat.* **75**, 419–433.

Connolly M. and Van Essen D. C. (1984) The representation of the visual field in parvicellular and magnocellular laminae of the lateral geniculate nucleus in the macaque monkey. *J. comp. Neurol.* In press.

Connolly M., Le Vay S. and Van Essen D. C. (1982) The complete pattern of ocular dominance stripes in macaque striate cortex. *Soc. Neurosci. Abstr.* **8**, 676.

Cooper M. L. and Pettigrew J. D. (1979) A neurophysiological determination of the vertical horopter in the cat and owl. *J. comp. Neurol.* **184**, 1–26.

Daniel P. M. and Whitteridge D. (1961) The representation of the visual field on the cerebral cortex in monkeys. *J. Physiol.* **159**, 203–221.

Donaldson I. M. L. and Whitteridge D. (1977) The nature of the boundary between cortical visual areas II and III in the cat. *Proc. R. Soc. Lond.* **199**, 445–462.

Dow B. M., Snyder R. G., Vautin R. G. and Bauer R. (1981) Magnification factor and receptive field size in foveal striate cortex of the monkey. *Expl Brain Res.* **44**, 213–228.

Filimonoff I. N. (1932) Uber die variabilitat der grosshirnrindenstruktur. Mitteilung II. Regio occipitalis beim erwachsenen Menshchen. *J. Psychol. Neurol.* **44**, 1–96.

Fischer B. (1973) Overlap of receptive field centers and representation of the visual field in the cat's optic tract. *Vision Res.* **13**, 2113–2120.

Gattass R., Gross C. G. and Sandell J. H. (1981) Visual topography of V2 in the macaque. *J. comp. Neurol.* **201**, 519–539.

Guld C. and Bertulis A. (1976) Representation of fovea in the striate cortex of vervet monkey, *Cercopithecus aethiops pygerythrus*. *Vision. Res.* **16**, 629–631.

Hendrickson A. E., Hunt S. P. and Wu J.-Y. (1981) Immunocytochemical localization of glutamic acid decarboxylase in monkey striate cortex. *Nature* **292**, 605–607.

Horton J. C. and Hubel D. H. (1980) Cytochrome oxidase stain preferentially labels intersection of ocular dominance and vertical orientation column in macaque striate cortex. *Soc. Neurosci. Abstr.* **6**, 315.

Hubel D. H. and Wiesel T. N. (1974) Uniformity of monkey striate cortex: a parallel relationship between field size, scatter, and magnification factor. *J. comp. Neurol.* **158**, 295–306.

Hubel D. H. and Freeman D. C. (1977) Projection into the visual field of ocular dominance columns in macaque monkey. *Brain Res.* **122**, 336–343.

Humphrey A. L. and Hendrickson A. E. (1980) Radial zones of high metabolic activity in squirrel monkey striate cortex. *Soc. Neurosci. Abstr.* **6**, 315.

Le Vay S., Hubel D. H. and Wiesel T. N. (1975) The pattern of ocular dominance columns in macaque visual cortex revealed by a reduced silver stain. *J. comp. Neurol.* **159**, 559–576.

Le Vay S., Connolly M., Houde J. and van Essen D. C. (1984) The complete pattern of ocular dominance stripes in the striate cortex and visual field of the macaque monkey. In preparation.

Malpeli J. G. and Baker F. H. (1975) The representation of the visual field in the lateral geniculate nucleus of *Macaca mulatta*. *J. comp. Neurol.* **161**, 569–594.

Maunsell J. H. R. and Van Essen D. C. (1983) Functional properties of neurons in the middle temporal visual area (MT) of the macaque monkey. I. Selectivity for stimulus direction, speed and orientation. *J. Neurophysiol.* **49**, 1127–1147.

Merzenich M. M., Kaas J. H., Sur M. and Lin C. S. (1978) Double representation of the body surface within cytoarchitectonic areas 3b and 1 in "SI" in the owl monkey (*Aotus trivirgatus*). *J. comp. Neurol.* **181**, 41–74.

Myerson J., Manis P. B., Miezin F. M. and Allman J. M. (1977) Magnification in striate cortex and the retinal ganglion cell layer of the owl monkey: a quantitative comparison. *Science* **198**, 855–857.

Poggio G. F. and Fischer B. (1977) Binocular interaction and depth sensitivity in striate and prestriate cortex of behaving rhesus monkey. *J. Neurophysiol.* **40**, 1392–1405.

Polyak S. (1957) *The Vertebrate Visual System*. Univ. of Chicago Press, Chicago, 1390 PP.

Rolls E. T. and Cowey A. (1970) Topography of the retina and striate cortex and its relationship to visual acuity in rhesus monkeys and squirrel monkeys. *Expl Brain Res.* **10**, 298–310.

Sakitt B. (1982) Why the cortical magnification factor in rhesus cannot be isotopic. *Vision Res.* **22**, 417–421.

Schwartz E. L. (1977) Spatial mapping in the primate sensory projection: analytic structure and relevance to perception. *Biol. Cybernet.* **25**, 181–194.

Schwartz E. L. (1980) Computational anatomy and functional architecture of striate cortex: a spatial mapping approach to perceptual coding. *Vision Res.* **20**, 645–669.

Stensaas S. S., Eddington D. K. and Dobelle W. H. (1974) The topography and variability of the primary visual cortex in man. *J. Neurosurg.* **40**, 747–755.

Sur M., Weller R. E. and Kaas J. H. 1980) Representation of the body surface in somatosensory area I of tree shrews, *Tupaia glis*. *J. comp. Neurol.* **194**, 71–95.

Sur M., Nelson R. J. and Kaas J. H. (1982) Representation of the body surface in cortical areas 3b and 1 of squirrel monkeys: comparison with other primates. *J. comp. Neurol.* **211**, 177–192.

Talbot S. A. and Marshall W. H. (1941) Physiological studies on neural mechanisms of visual localization and discrimination. *Am. J. Ophthal.* **24**, 1255–1264.

Tootell R. B. H., Silverman M. S., Switkes E. and De Valois R. L. (1982) Deoxyglucose analysis of retinotopic organization in primate striate cortex. *Science* **218**, 902–904.

Tusa R. J., Palmer L. A. and Rosenquist A. C. (1978) The retinotopic organization of area 17 (striate cortex) in the cat. *J. comp. Neurol.* **177**, 213–236.

Tusa R. J., Rosenquist A. C. and Palmer L. A. (1979) Retinotopic organization of areas 18 and 19 in the cat. *C. comp. Neurol.* **185**, 657–678.

Van Essen D. C. and Maunsell J. H. R. (1980) Two-dimensional maps of the cerebral cortex. *J. comp. Neurol.* **191**, 255–281.

Van Essen D. C., Maunsell, J. H. R. and Bixby J. L. (1981) The middle temporal visual area in the macaque: myeloarchitecture, connections, functional properties and topographic organization. *J. comp. Neurol.* **199**, 293–326.

Van Essen D. C., Newsome W. T. N. and Bixby J. L. (1982) The pattern of interhemispheric connections and its relationship to extrastriate visual areas in the macaque monkey. *J. Neurosci.* **2**, 265–283.